Supplementary Information for

High-dimensional mass cytometry analysis of NK cell alterations in Acute Myeloid Leukemia identifies a subgroup with adverse clinical outcome

Anne-Sophie Chretien, Raynier Devillier, Samuel Granjeaud, Charlotte Cordier, Clemence Demerle, Nassim Salem, Julia Wlosik, Florence Orlanducci, Laurent Gorvel, Stephane Fattori, Marie-Anne Hospital, Jihane Pakradouni, Emilie Gregori, Magali Paul, Philippe Rochigneux, Thomas Pagliardini, Mathieu Morey, Cyril Fauriat, Nicolas Dulphy, Antoine Toubert, Herve Luche, Marie Malissen, Didier Blaise, Jacques A. Nunès, Norbert Vey, and Daniel Olive.

Corresponding author:
Dr. Anne-Sophie Chretien
anne-sophie.chretien@inserm.fr

This PDF file includes:

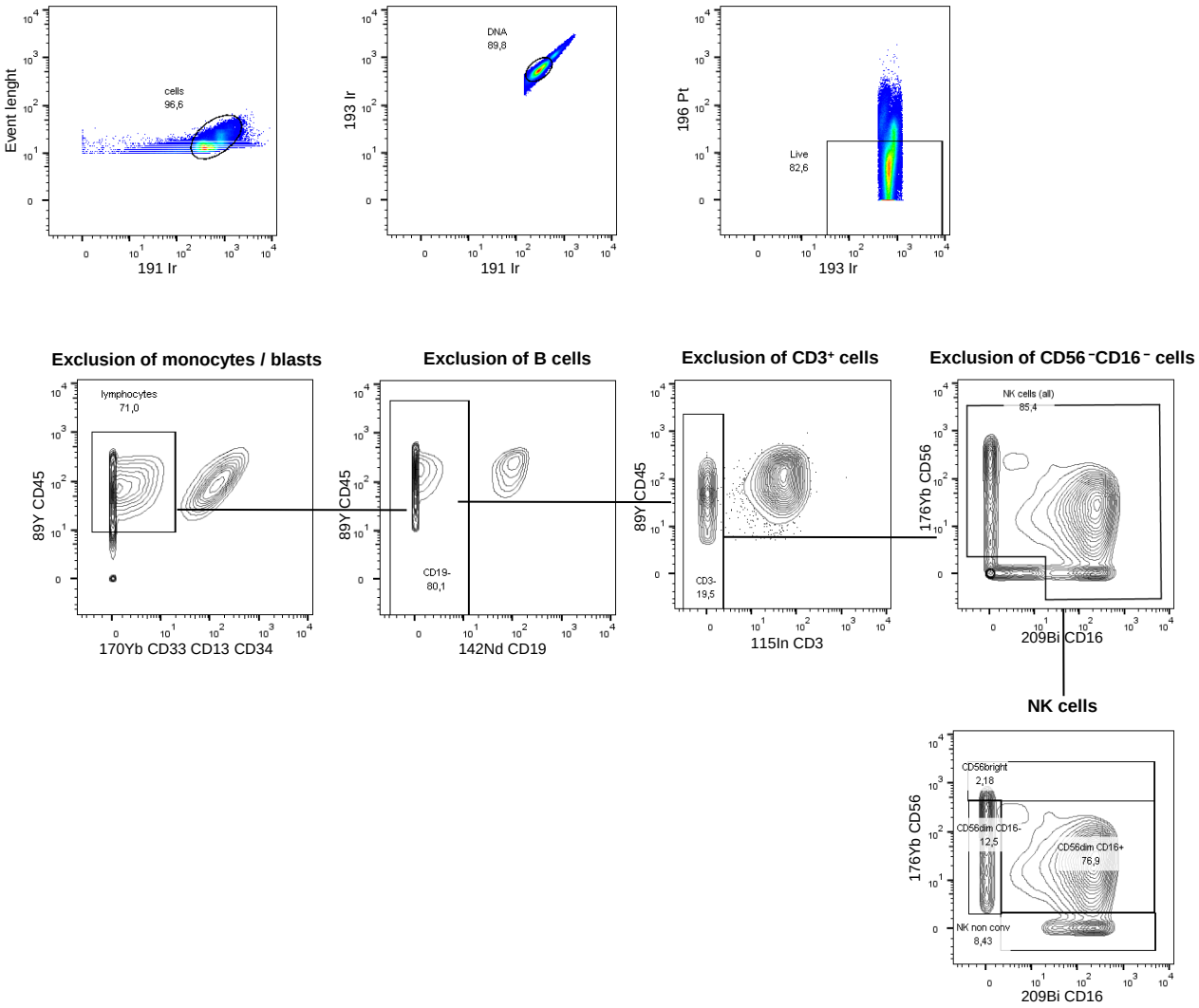

Supplementary Figure 1. Gating strategy. PBMCs from HV and patients with AML were stained with the indicated set of antibodies (see Supplementary Table 1) and analyzed by mass cytometry (CyTOF Helios®). After removal of beads, cells were pre-gated as DNA^+, cisplatin$^-$ cells. Monocytes and leukemic blasts were excluded based on expression of CD13, CD33, and CD34 and on low or absent CD45 expression; B cells and T cells were excluded based on CD19 and CD3 expression, respectively. Four subsets of NK cells were defined based on CD56 and CD16 expression: $CD56^{bright}$ NK cells, $CD56^{dim}CD16^+$ NK cells, $CD56^{dim}CD16^-$ NK cells, and unconventional $CD56^-CD16^+$ NK cells.

OS

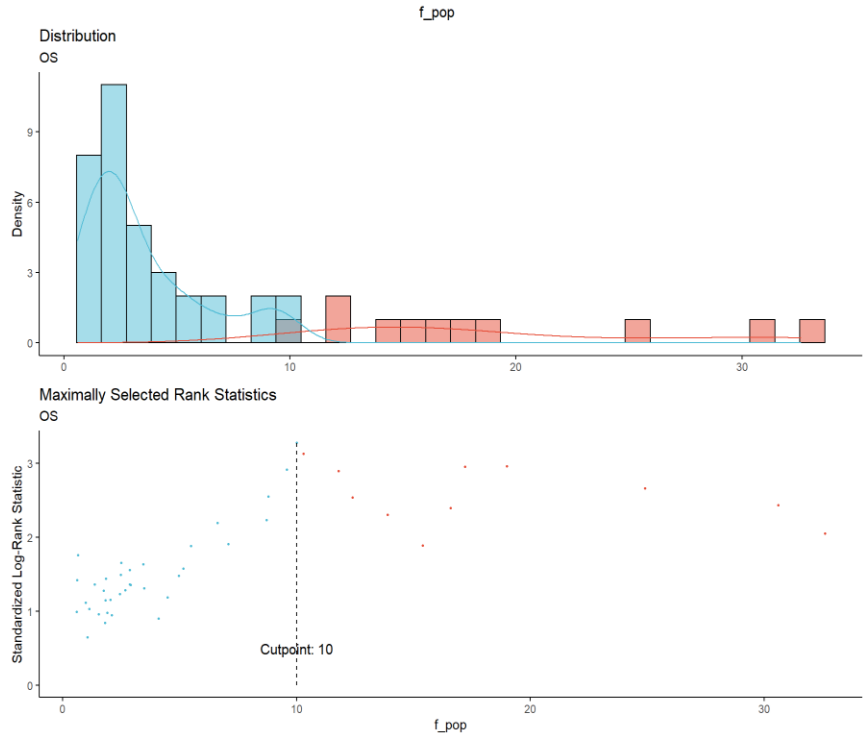

RFS

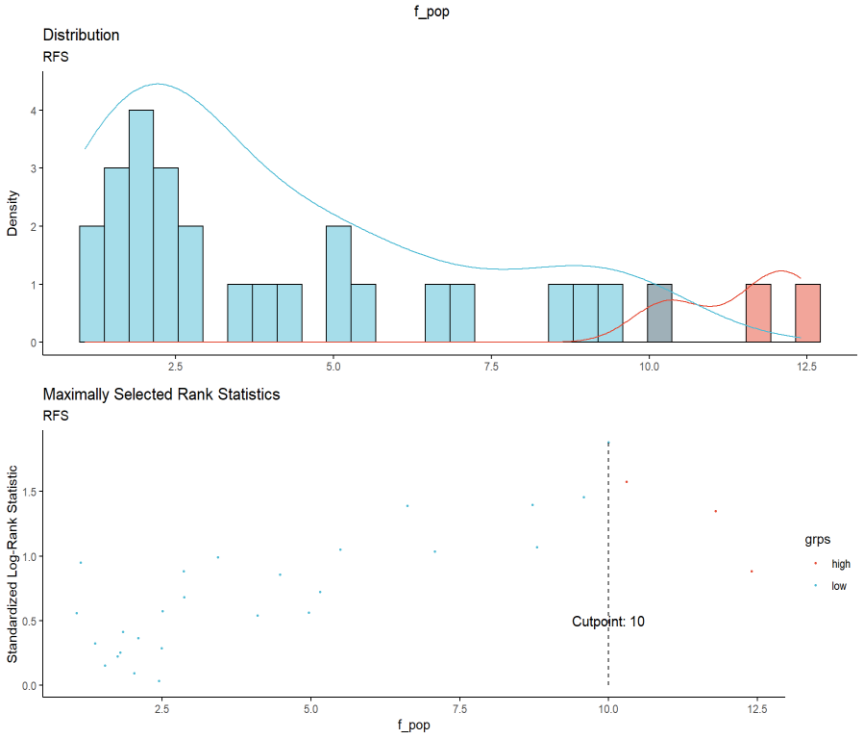

Supplementary Figure 2. Threshold determination for definition of AML subgroups. The optimal cut-points were determined using maximally selected log-rank statistics using the maxstat R package. Maxstat enables identification of, for a given prognostic parameter, the optimal threshold that best discriminates two groups of patients. (https://cran.r-project.org/web/packages/maxstat/index.html)

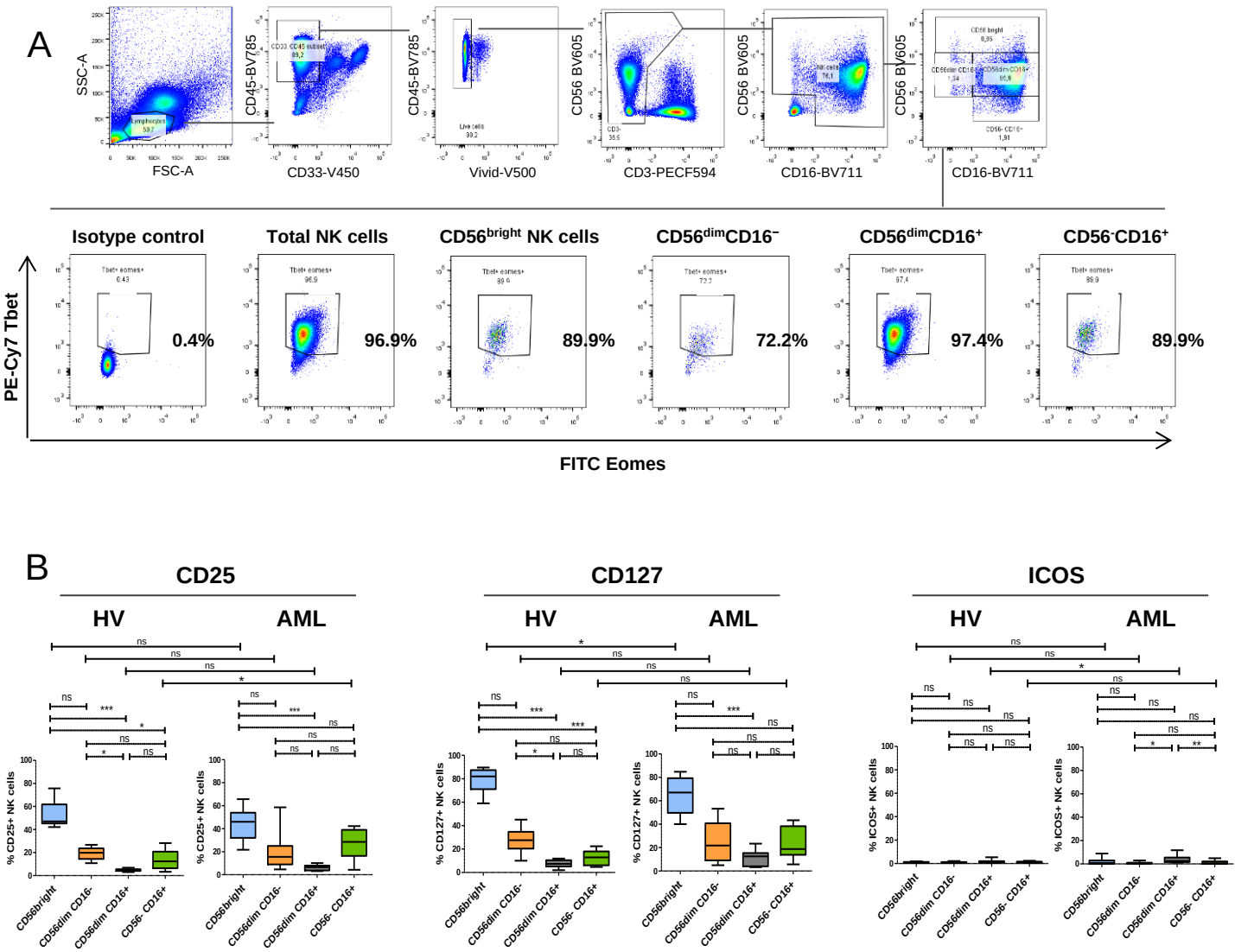

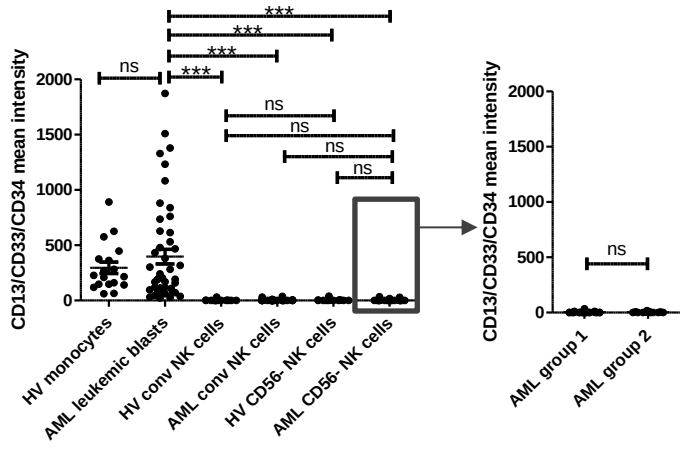

Supplementary Figure 3. ILC and leukemic markers expression by CD3$^-$CD56$^-$CD16$^+$ cells. (A) NK cells from HV were analyzed by flow cytometry to assess expression of Tbet and Eomes in the subset of CD56$^-$CD16$^+$ NK cells. (B) Expression of ILC1 markers (CD25, CD127, and ICOS) was further assessed by mass cytometry in peripheral NK cells from HV and from patients with AML. (C) Mean CD13/CD33/CD34 intensity in conventional and CD56$^-$CD16$^+$ NK cells. Differences between clusters were assessed using a Friedman test followed by a Dunn's test. Differences between HV and AML patients were performed using a 2-tailed Mann-Whitney test. *: P<0.05; **: P<0.01; ***: P<0.001; ns: non-significant.

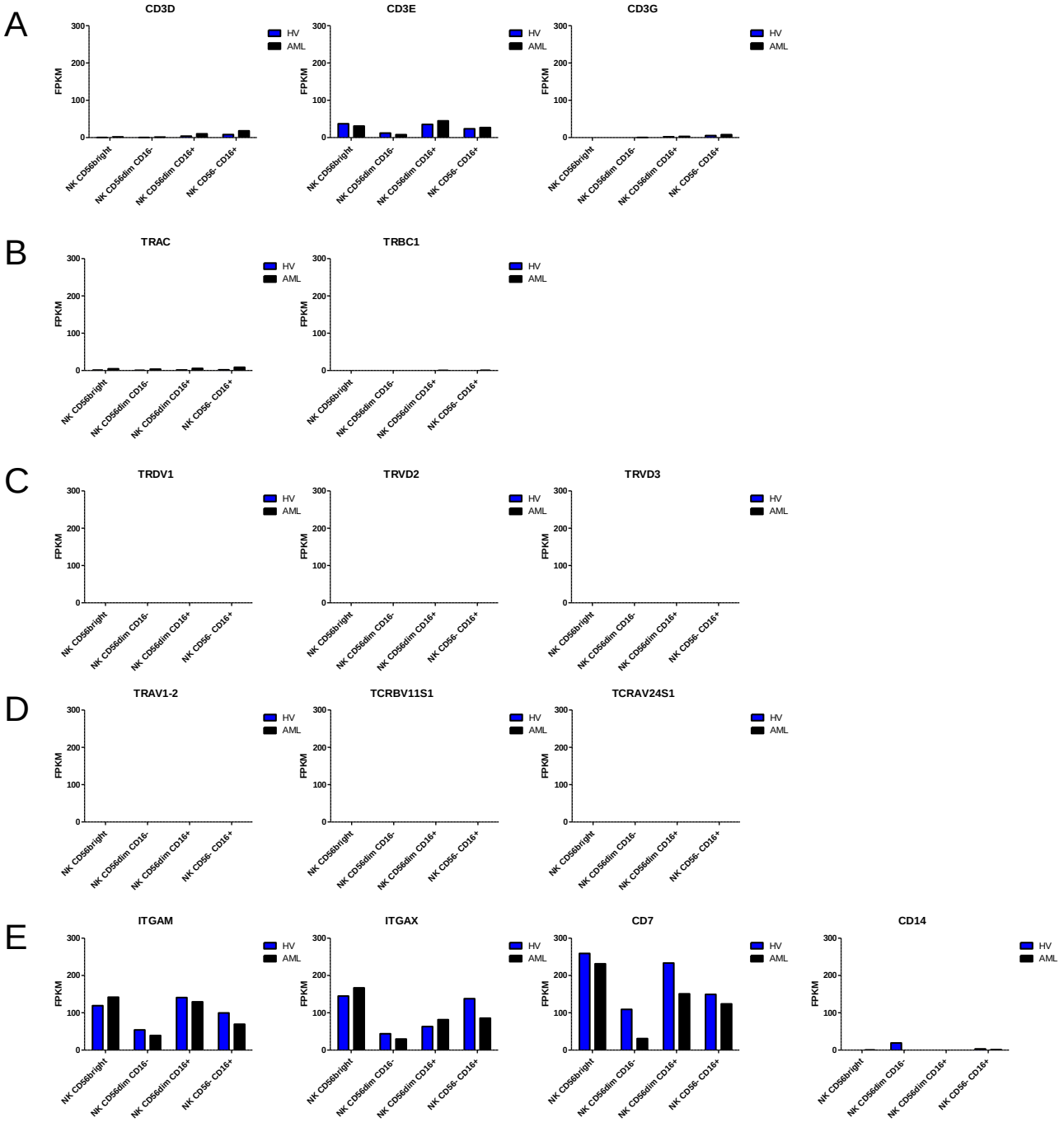

Supplementary Figure 4. Absence of expression of genes transcripts of conventional T cells, γδ T cells, MAIT and iNKT by CD56^{-}CD16^{+} NK cells. CD56^{bright}, CD56^{dim}CD16^{+}, CD56^{dim}CD16^{-} and CD56^{-}CD16^{+} were sorted using a FACSAria III cell sorter. The barplots display the expression levels of transcripts of genes coding CD3δ, CD3ε and CD3γ (A), genes coding TCRα and TCRβ (B), genes specific of γδ T cells (C), MAIT, iNKT (D), and genes discriminating monocytes/DC-like cells from unconventional NK cells (E). FPKM: fragments per kilobase of transcript per million mapped reads; iNKT: invariant NKT cells; MAIT: mucosal-associated invariant T cells.

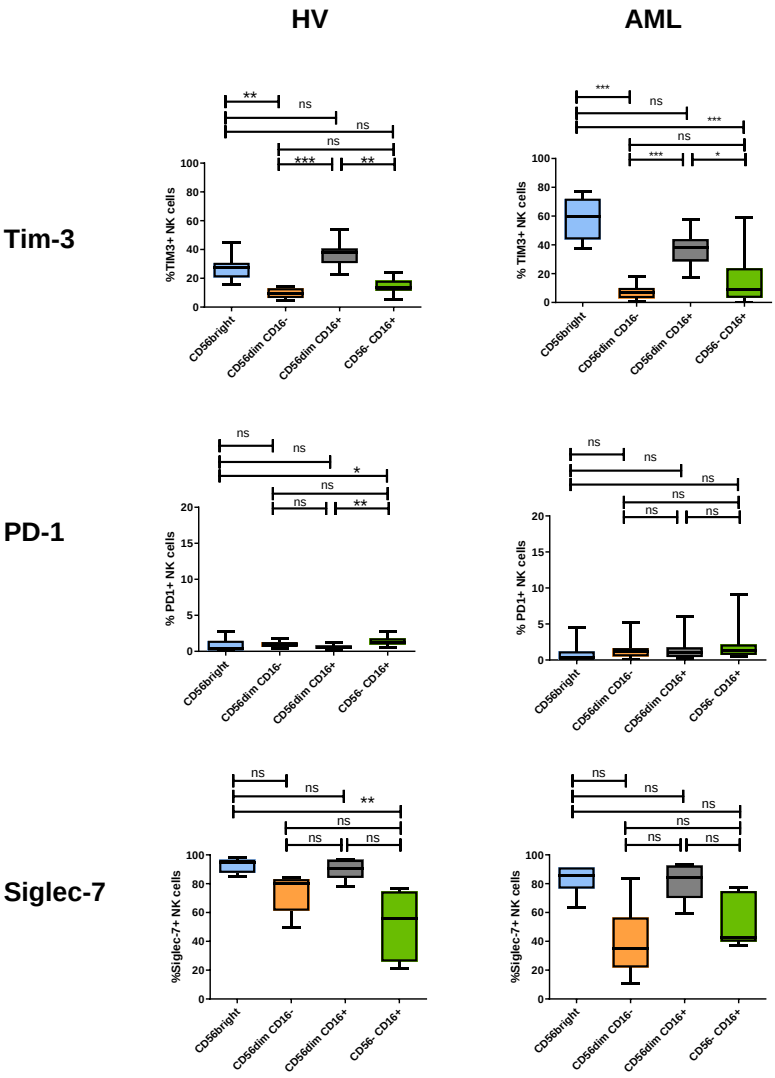

Supplementary Figure 5. Tim-3, PD-1 and Siglec-7 expression by NK cell subset. Markers of NK cell exhaustion (Tim-3 and PD-1) were assessed by mass cytometry. Siglec-7 expression was assessed by flow cytometry. Data were analyzed using a Kruskal-Wallis test followed by a Dunn's test. Results are presented as interquatile ranges, median, and whiskers from minimum to maximum. *: P<0.05; **: P<0.01; ***: P<0.001; HV: healthy volunteer; ns: non-significant.

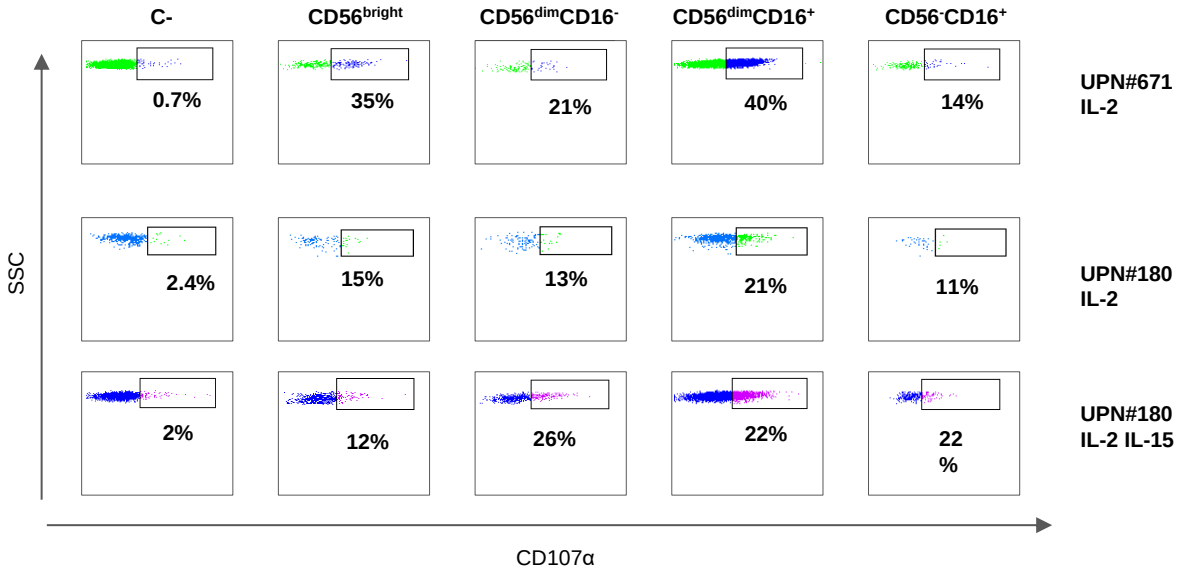

Supplementary Figure 6. CD56^{-}CD16^{+} NK cells respond to K562 target cells. CD56^{bright}, CD56^{dim}CD16^{-}, CD56^{dim}CD16^{+} and CD56-CD16+ NK cells from AML patients were sorted using a cell sorter and incubated overnight with IL-2 100UI/mL or IL-2 100UI/mL and IL-15 10ng/mL, and co-cultured with K562 target cells. CD107α expression was assessed by flow cytometry. C-: negative control; UPN, unique patient number.

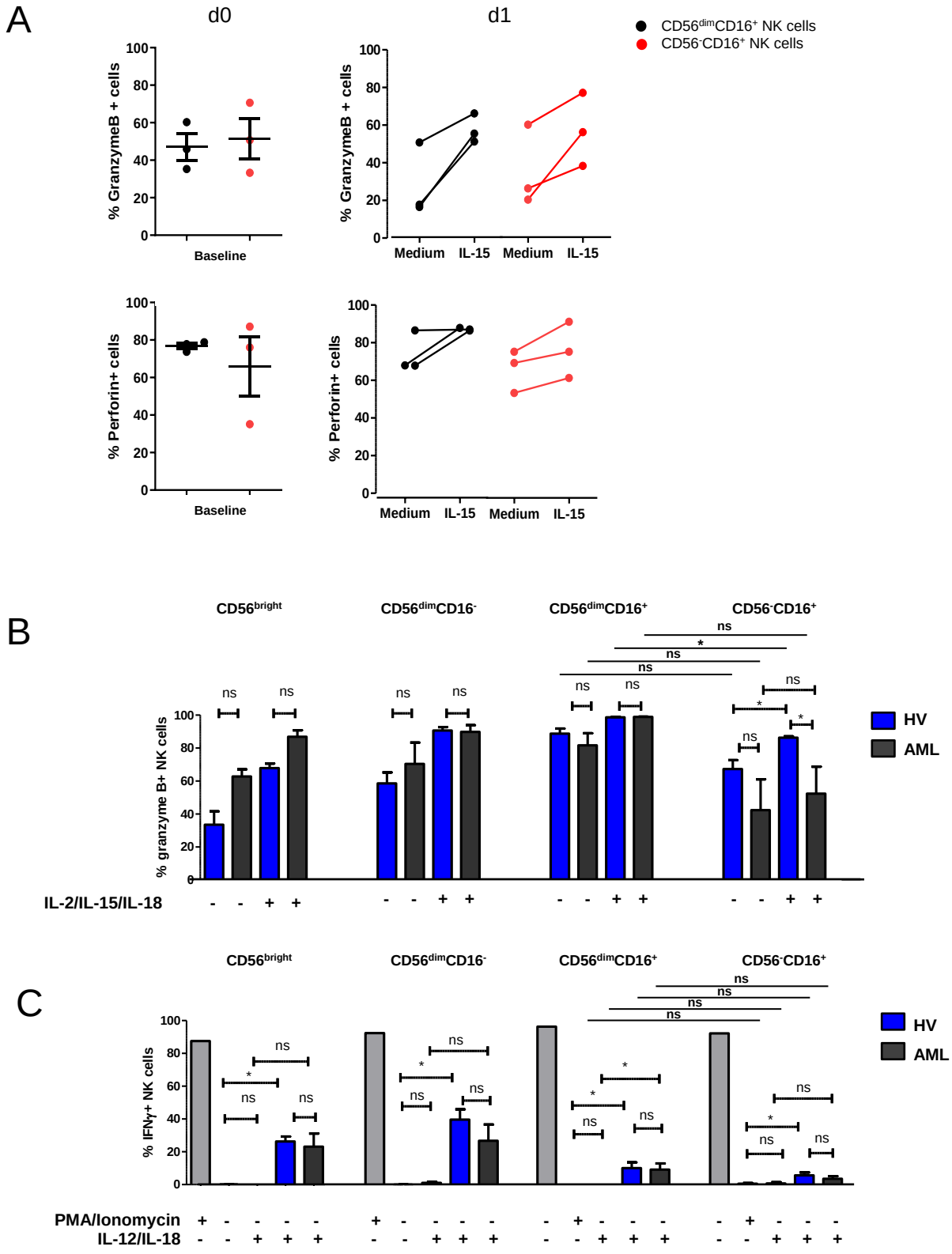

Supplementary Figure 7. CD56$^-$CD16$^+$ NK cells respond to cytokinic stimulation. A. PBMC from AML patients (N=3) were incubated with or without IL-15 10ng/mL. Perforin and Granzyme B expression were assessed by flow cytometry at day baseline (left panel) and at day 1 (right panel). B. PBMC from healthy volunteers (N=4) and AML patients (N=3) were incubated with IL-2 100IU/mL or a combination of IL-2 100IU/mL, IL-15 10ng/mL and IL-18 100ng/mL. Granzyme B expression was assessed after overnight incubation. C. PBMC from healthy volunteers (N=4) and AML patients (N=3) were incubated with IL-2 100IU/mL, IL-12 10ng/mL, IL-18 100ng/mL. IFNγ expression was assessed after 6 hours of incubation.

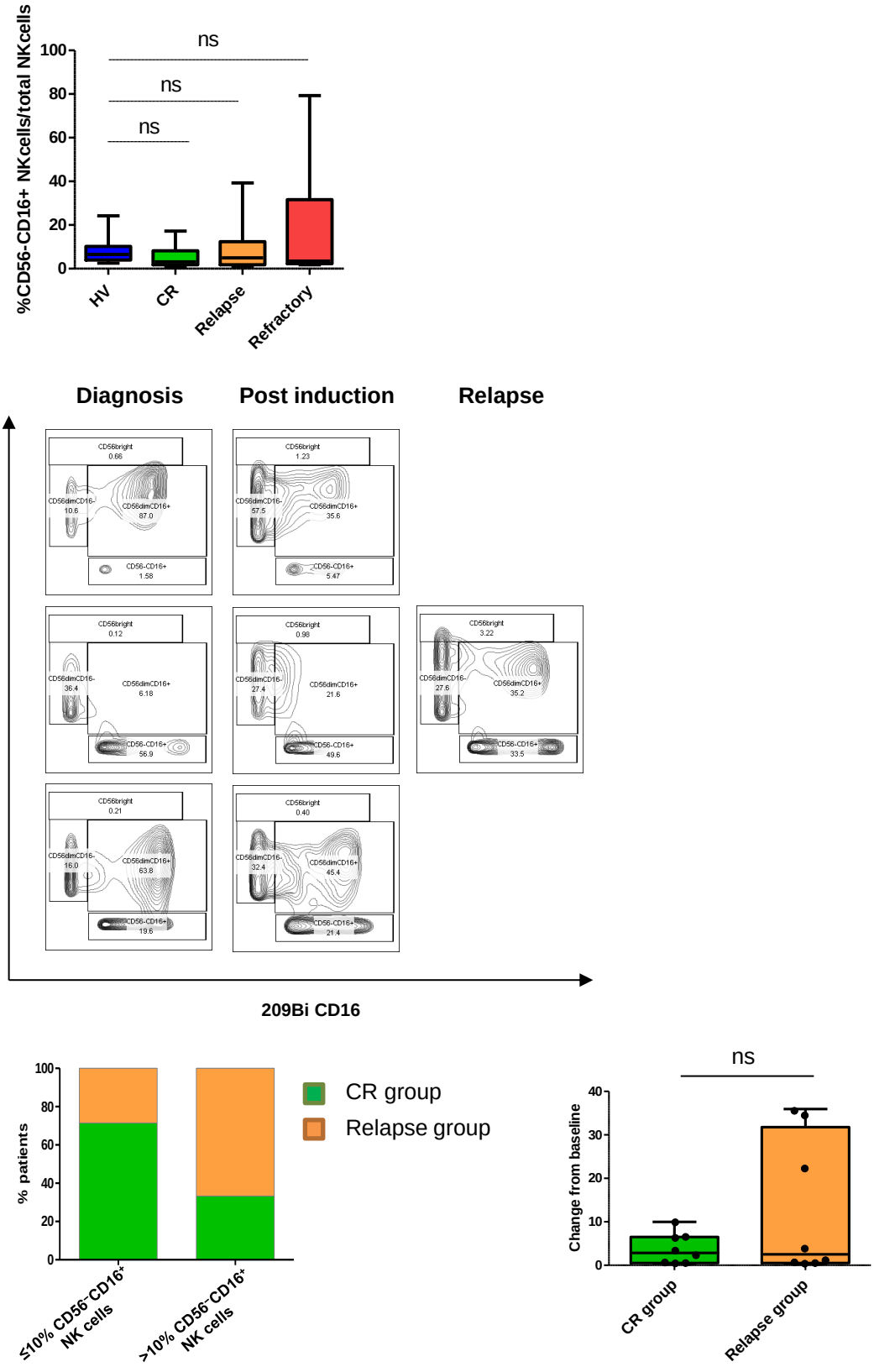

Supplementary Figure 8. Induction chemotherapy does not restore non-pathological frequency of CD56^{-}CD16^{+} NK cells. Upper panel: the frequency of CD56^{-}CD16^{+} NK cells CD56 was assessed according to clinical outcome. Middle panel: when paired samples were available, the frequency of CD56^{-}CD16^{+} NK cells was assessed at diagnosis and 30 to 45 days after induction therapy (n=16). Lower panel: raw frequencies at the time of complete remission and change from baseline (diagnosis vs complete remission) were analyzed by subgroups of patients defined according to clinical outcome. The change from baseline was calculated as the ratio between the frequency of CD56^{-}CD16^{+} NK cells at diagnosis and the frequency of CD56^{-}CD16^{+} NK cells at complete remission (CR). HV: healthy volunteer; ns, non-significant; UPN, unique patient number.

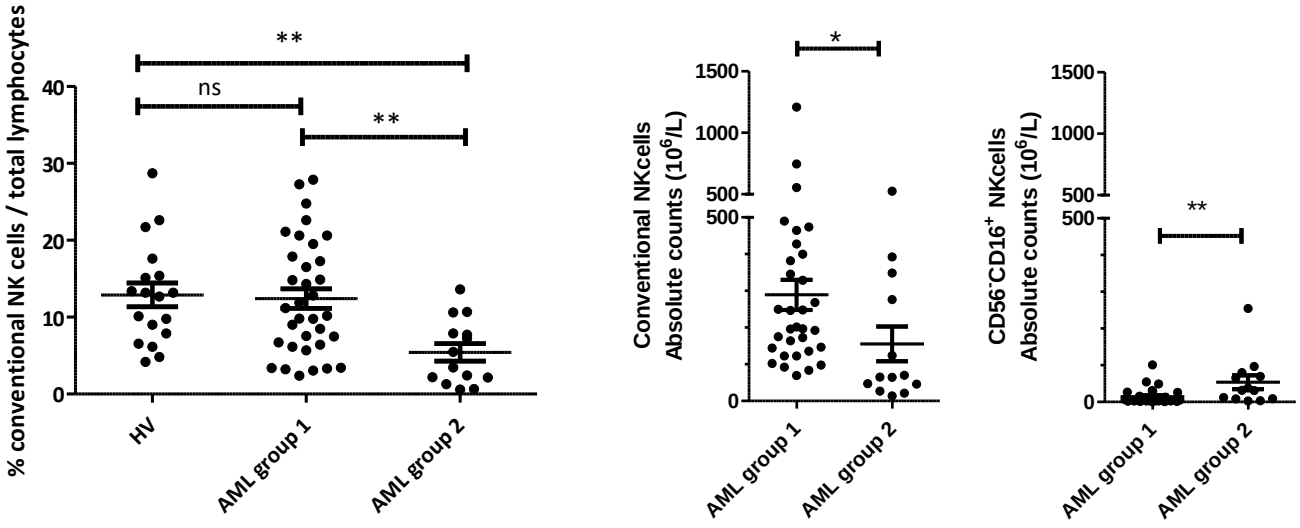

Supplementary Figure 9. High frequency of $CD56^{-}CD16^{+}$ NK cells is associated with a decrease of conventional NK cells. Frequencies (left panel) and absolute counts of conventional $CD56^{+}$ NK cells (middle panel) and $CD56^{-}CD16^{+}$ NK cells were determined using manual gating and compared between healthy volunteers, patients with low frequencies of $CD56^{-}CD16^{+}$ NK cells (group 1) and patients with high frequencies of $CD56^{-}CD16^{+}$ NK cells (group 2). Results are presented as mean ± SEM. For multiple comparisons, data were analyzed using a Kruskal–Wallis test followed by a Dunn's post-test; comparisons between two groups were performed using a 2-tailed Mann-Whitney test.*: P<0.05 **: P<0.01; ns: non-significant.

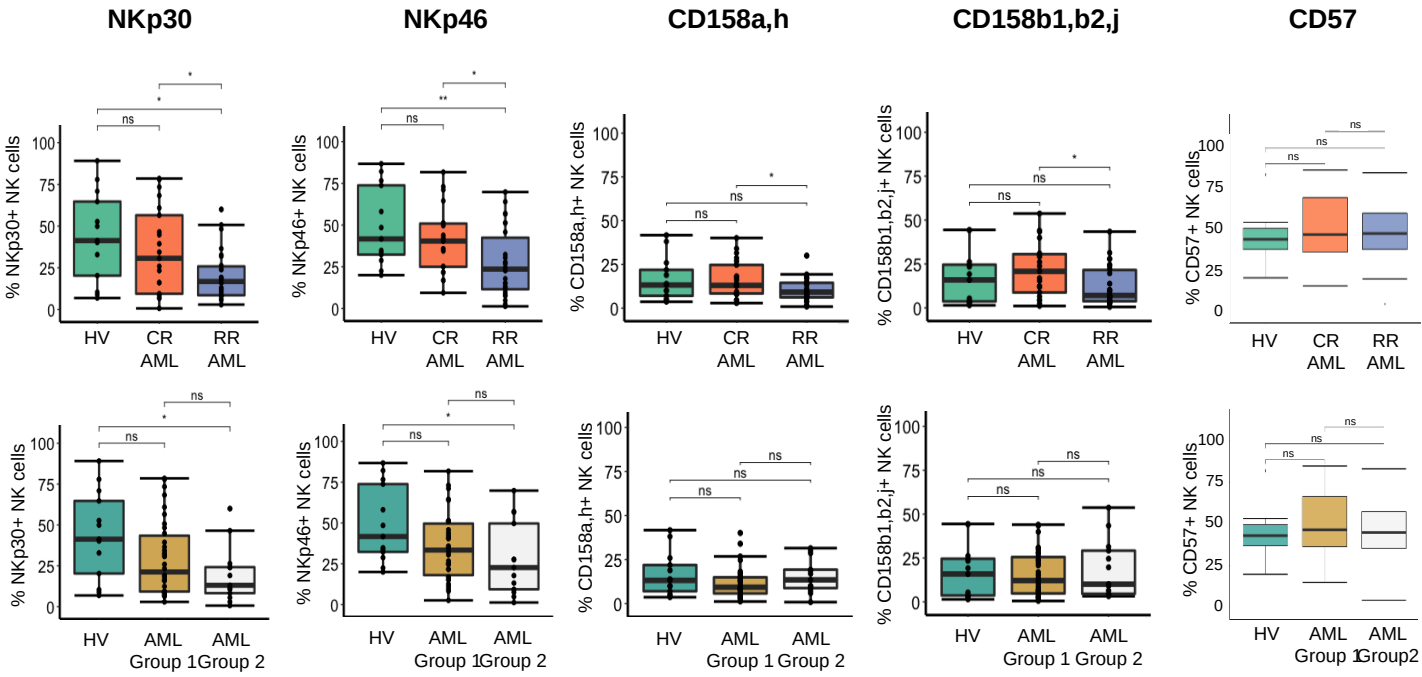

Supplementary Figure 10. NCR and NK cell maturation markers by AML subgroup. The frequency of NKp30$^+$, NKp46$^+$, KIR$^+$ and CD57$^+$ NK cells was assessed on conventional NK cells and analyzed according to clinical outcome (upper panel) or AML group (lower panel). Results are presented as mean ± SEM. Data were analyzed using a Kruskal–Wallis test followed by a Dunn's post-test.*: P<0.05 **: P<0.01; ns: non-significant.

Supplementary Table 1. Mass cytometry panels

Panel 1

Antigen	Metal/fluorochrome		Company
CD45	89Y	Extracellular	Fluidigm
CD3	115In	Extracellular	CRCM*
TCRVd2	141Pr	Extracellular	Beckman Coulter*
CD19	142Nd	Extracellular	Fluidigm
CD45RA	143Nd	Extracellular	Fluidigm
CD4	145Nd	Extracellular	Fluidigm
CD8a	146Nd	Extracellular	Fluidigm
BCL-2	150Nd	Intracellular	Cell Signaling*
NKG2C	152Sm	Extracellular	Miltenyi
TCRpangd	153Eu	Extracellular	Miltenyi
CD158b1/b2j	154Sm	Extracellular	Beckman Coulter*
CD27	155Gd	Extracellular	Fluidigm
BCL-Xl	158Gd	Intracellular	Cell Signaling*
Ki-67	159Tb	Intracellular	BioLegende
NKG2D	160Gd	Extracellular	Beckman Coulter
NKp46	162Dy	Extracellular	Fluidigm
DNAM-1	164Dy	Extracellular	Beckman Coulter*
NKG2A	165Ho	Extracellular	Beckman Coulter*
CD96	166Er	Extracellular	BioLegende
CD158a/h	168Er	Extracellular	Beckman Coulter*
NKp30	169Tm	Extracellular	Beckman Coulter*
CD57	172Yb	Extracellular	Fluidigm
CD56	176Yb	Extracellular	Fluidigm
CD16	209Bi	Extracellular	Fluidigm
CD34	PE/biotinylated	Extracellular	Beckman Coulter*/Sigma*
CD13	PE/biotinylated	Extracellular	BD Biosciences*/Sigma*
CD33	PE/biotinylated	Extracellular	Beckman Coulter*/Sigma*
Anti-PE	156Gd	Extracellular	Fluidigm

* Indicates purified antibodies labeled with a Maxpar® antibody labeling kit

Panel 2

Antigen	Metal/fluorochrome		Company
CD45	89Y	Extracellular	Fluidigm
CD3	115In	Extracellular	CRCM*
Ki-67	141Pr	Intracellular	BioLegende
CD45RA	143Nd	Extracellular	Fluidigm
HVEM	144Nd	Extracellular	Fluidigm
CD8a	146Nd	Extracellular	Fluidigm
CD25	149Sm	Extracellular	Fluidigm
OX-40	150Nd	Extracellular	Fluidigm
ICOS	151Eu	Extracellular	Fluidigm
TIM-3	153Eu	Extracellular	Fluidigm
TIGIT	154Sm	Extracellular	Fluidigm
PD-1	155Gd	Extracellular	Fluidigm
PD-L1	156Gd	Extracellular	Fluidigm
4-1BB	158Gd	Extracellular	Fluidigm
CCR7	159Tb	Extracellular	Fluidigm
CD28	160Gd	Extracellular	Fluidigm
CTLA-4	161Dy	Intracellular	Fluidigm
FOXP3	162Dy	Intracellular	Fluidigm
BTLA	163Dy	Extracellular	Fluidigm
CD95	164Dy	Extracellular	Fluidigm
CD127	165Ho	Extracellular	Fluidigm
CD44	166Er	Extracellular	Fluidigm
CD27	167Er	Extracellular	Fluidigm
CD69	168Er	Extracellular	Fluidigm
TCRVd2	169Tm	Extracellular	Fluidigm
DNAM-1	171Yb	Extracellular	Fluidigm
CD57	172Yb	Extracellular	Fluidigm
LAG3	175Lu	Extracellular	Fluidigm
CD56	176Yb	Extracellular	Fluidigm
CD16	209Bi	Extracellular	Fluidigm
CD34	PE	Extracellular	Beckman Coulter*/Sigma*
CD13	PE	Extracellular	BD Biosciences*/Sigma*
CD33	PE	Extracellular	Beckman Coulter*/Sigma*
Anti-PE	156Gd	Extracellular	Fluidigm

* Indicates purified antibodies labeled with a Maxpar® antibody labeling kit